

Vibrational properties of amorphous silicon-germanium alloys and superlattices

A. M. Bouchard

*Microelectronics Research Center, Iowa State University, Ames, Iowa 50011
and Ames Laboratory, U.S. Department of Energy, Iowa State University, Ames, Iowa 50011*

R. Biswas

Microelectronics Research Center, Iowa State University, Ames, Iowa 50011

W. A. Kamitakahara

Ames Laboratory, U.S. Department of Energy, Iowa State University, Ames, Iowa 50011

G. S. Grest

Corporate Research Science Laboratory, Exxon Research and Engineering Company, Annandale, New Jersey 08801

C. M. Soukoulis

*Microelectronics Research Center, Iowa State University, Ames, Iowa 50011
and Ames Laboratory, U.S. Department of Energy, Iowa State University, Ames, Iowa 50011*

(Received 18 April 1988)

Densities of states and localization characteristics have been calculated for vibrational modes in $a\text{-Si}_x\text{Ge}_{1-x}$ alloys and $a\text{-Si}/a\text{-Ge}$ superlattices, using amorphous tetrahedral networks generated by molecular-dynamics methods. For the alloys, the calculated densities of states agree very well with Raman scattering experiments at all concentrations $0 \leq x \leq 1$. We explicitly show that an x -dependent feature at 390 cm^{-1} arises primarily from Si—Ge bond-stretching motions. The localization of vibrational modes is enhanced in magnitude and in frequency range for the alloys as compared with the pure amorphous materials, but extended modes are still present at all x . To account for the Raman measurements on thin $a\text{-Si}/a\text{-Ge}$ superlattices, a mixed Si-Ge interfacial region about 5 \AA in thickness is indicated by our calculations.

I. INTRODUCTION

Disorder strongly affects the excitation spectra of solids. In this paper we study the combined effects of structural disorder, mass disorder, and the presence of interfaces on the vibrational spectra of a two-component alloy system. In particular, we have examined models of amorphous $\text{Si}_x\text{Ge}_{1-x}$ alloys and $a\text{-Si}/a\text{-Ge}$ superlattices. These are important materials for microelectronics and photovoltaic applications, and the atomic structure and defect properties play an important role in applications. In this paper we study basic questions regarding the vibrational spectra of these materials which are an important probe of the local atomic structure.

Raman scattering spectra in amorphous $\text{Si}_x\text{Ge}_{1-x}$ alloys have been extensively investigated by Lannin^{1,2} and Shevchik *et al.*³ The most noteworthy feature of the experimental data¹ is the appearance of a new vibrational band at $\sim 390 \text{ cm}^{-1}$ in the alloy densities of states (DOS) that is absent in either of the pure amorphous materials. This band was interpreted¹ as due to Si—Ge bond-stretching motions. Our calculations of the DOS for the alloys explicitly support this interpretation. Raman measurements of $a\text{-Si}/a\text{-Ge}$ superlattices performed by Persans *et al.*,^{4,5} demonstrated that for large superlattice periods ($d_s > 40 \text{ \AA}$), the spectra were weighted sums of the contributions of the $a\text{-Si}$ and $a\text{-Ge}$ layers. For thin

superlattices ($d_s < 30 \text{ \AA}$), a vibrational band at 370 cm^{-1} was present, similar to the Si—Ge bond-stretching feature of the alloy. These alloylike spectra were interpreted^{4,5} in terms of an intermixing of the Si and Ge atoms in regions of approximately one monolayer thickness at the interfaces. We calculate the DOS for thin superlattices in this paper and examine this interpretation closely, by performing DOS calculations for roughened interfaces of various widths.

In this paper we make use of $a\text{-Si}$ models that were computer generated by molecular-dynamics calculations,⁶ using two- and three-body interatomic silicon potentials.⁷ The quenching of a melt of bulk silicon resulted in an amorphous silicon structure that had radial distribution functions and bond-angle distributions that compared well with experiment and other theoretical models. The vibrational properties of the molecular-dynamics-generated $a\text{-Si}$ models were calculated in a recent paper,⁸ and the phonon DOS were found to agree very well with both experiment,⁹ and with those of another $a\text{-Si}$ model generated with Monte Carlo methods by Wooten, Weaire, and Winer.¹⁰ Novel low-frequency quasilocalized resonant-vibrational states were found⁸ that primarily involved vibrations of undercoordinated atoms. In addition, localized vibrations were also found at the high-frequency band edge. In this paper we study how the localization characteristics at both low and high frequen-

cies are affected by the mass disorder in the $\text{Si}_x\text{Ge}_{1-x}$ alloy. Similar calculations for the superlattices show that the high-frequency localized modes are primarily confined to the amorphous interface.

II. THEORETICAL MODEL

The structural models of amorphous silicon (*a*-Si) adopted for this study were generated by molecular-dynamics (MD) simulations using the separable two- and three-body interatomic potentials recently developed by Biswas and Hamann.⁷ Amorphous structures consisting of $N = 216, 512,$ and 2000 atoms with periodic boundary conditions were produced by Biswas, Grest, and Soukoulis⁶ (BGS) by simulating a quench from the melt of bulk crystalline silicon, freezing in disorder which is characteristic of the amorphous phase. The resulting *a*-Si networks have static structural features that compare well with experiment.^{8,9} Most of the calculations in this paper are based on the 512-atom and 216-atom BGS *a*-Si models.

An important difference between the BGS models and *a*-Si models generated by Monte Carlo methods by Wooten, Weaire, and Winer^{10,11} (WWW), is the presence, in the former, of coordination defects, consisting mainly of threefold- and fivefold-coordinated atoms. All atoms of the WWW *a*-Si model were fourfold coordinated. Our 512-atom network has 52 atoms which are fivefold bonded, 34 atoms which are threefold bonded, and a single twofold-bonded atom. As we have discussed in detail in a separate paper,⁸ the undercoordinated atoms in the BGS models for *a*-Si give rise to a novel feature, a number of highly localized low-frequency vibrations. Coordination defects have also been found in *a*-Si models generated with similar techniques by Luedtke and Landman,¹² and Kluge, Ray, and Rahman,¹³ as well as by Car and Parrinello¹⁴ in simulated annealing methods combining first-principles calculations with molecular dynamics. The BGS *a*-Si model has a rms bond-angle deviation of 11.6° and a rms bond-length deviation of 1.9% of the *c*-Si bond length in comparison to corresponding values of 10.8° and 1.9% for the WWW *a*-Si model.

Clearly, the BGS models have defect concentrations that exceed experimental estimates for device quality *a*-Si. However, it is much easier to understand the properties of these defects when they are present in our calculation at high concentrations, and we expect their characteristics would be similar at small concentrations, incorporating some properties that pertain to real *a*-Si films produced under various nonequilibrium conditions. The coordination defects led to new localized vibrational modes at low frequencies and an enhancement of the localization at high frequencies. The conclusions in this paper on the vibrational DOS and the high-frequency localization properties were insensitive to the defect properties, since they were found with both the BGS model, and the WWW model that had no coordination defects.

The potential used in the MD calculation for creating the BGS structural model is somewhat more complicated than is necessary for calculating vibrational properties, and its parameters were not optimized to fit vibrational

data. For the present purposes of determining phonon densities of states, we adopted the Keating model,¹⁵ in which the potential energy of the system is defined by

$$V = \frac{3}{16}(\alpha/d^2) \sum_{l,i} (\mathbf{r}_{li} \cdot \mathbf{r}_{li} - d^2)^2 + \frac{3}{8}(\beta/d^2) \sum_{l,i(i \neq j)} (\mathbf{r}_{li} \cdot \mathbf{r}_{lj} + d^2/3)^2, \quad (1)$$

as the most convenient choice for calculating vibrational spectra. Here \mathbf{r}_{li} is the vector distance from atom l to its i th neighbor, and d is the crystalline equilibrium bond length, $d = 2.3516 \text{ \AA}$. The two parameters that enter the Keating model are the bond-stretching force constant α and the bond-bending force constant β . It was necessary to perform an additional relaxation of the BGS network with the Keating potential, using Monte Carlo calculations at zero temperature. The change in the atomic positions were minimal as a result of this additional relaxation step, which led to a local minimum of the Keating potential energy. The structural volumes were also varied, producing a relaxed *a*-Si structure with density 9.6% greater than the crystal. The dynamical matrix was constructed both from analytic derivatives of (1) and numerically from differences in strain energy at relaxed atomic positions and at slightly displaced positions. Diagonalization of the dynamical matrix produced the normal-mode frequencies, eigenvectors, and densities of states $g(\omega)$.

The values we used for the Keating parameters, $\alpha = 42.1 \text{ N/m}$ and $\beta/\alpha = 0.16$, give $g(\omega)$ for the BGS *a*-Si networks in good agreement with neutron-scattering data⁹ (Fig. 1). The same values also give good results for the crystal $g(\omega)$. The values originally chosen by Keating to fit the elastic constants of crystalline Si ($\alpha = 48.5 \text{ N/m}$, $\beta/\alpha = 0.285$) do not reproduce $g(\omega)$ for either crystalline or amorphous Si in a satisfactory manner as seen from Fig. 5 in Ref. 6, and as also noted by Ishii *et al.*¹⁶ To model the $g(\omega)$ satisfactorily, a substantial softening of the bond-bending force constant β from the Keating value, similar to that used in this paper, was

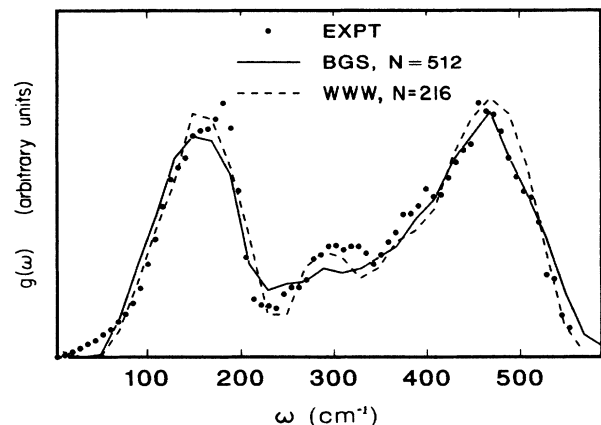


FIG. 1. Vibrational densities of states for *a*-Si models obtained by molecular-dynamics methods (BGS) and Monte Carlo methods (WWW), compared with neutron-scattering data.

used by Ishii *et al.*¹⁶ for *a*-Si and Baraff *et al.*¹⁷ for *c*-Si.

As a further test of our procedures, including our choice of Keating parameters, we calculated $g(\omega)$ for another *a*-Si structure that contained only fourfold-coordinated atoms, which was constructed by Wooten, Winer, and Weaire¹⁰ from Monte Carlo simulations. Monte Carlo bond switching rearrangements were used to disorder the diamond structure, so that distorted tetrahedral coordination was preserved for all atoms, but fivefold and sevenfold rings were introduced. The $g(\omega)$ for the WWW model (Fig. 1) also agrees well with neutron data.

With a view to modeling amorphous silicon-germanium systems, we extended this vibrational model to amorphous germanium using the same *a*-Si networks. The parameters $\alpha=39$ N/m with the same $\beta/\alpha=0.16$ bond-bending force constant, together with the heavier Ge mass, gave good quantitative agreement between the calculated *a*-Ge vibrational DOS and experiment, qualitatively similar to that for *a*-Si shown in Fig. 1. The equilibrium *c*-Ge bond length was taken to be the same as for Si, in the calculation. The very similar force constants α and β for Si and Ge imply that the *a*-Ge vibrational properties may be obtained by scaling the *a*-Si spectrum by a factor that is slightly smaller than the square root of the mass ratio of Si to Ge. This is in keeping with the observation that the phonon dispersion curves, normalized to the ion-plasma frequency, are nearly identical for *c*-Si and *c*-Ge,^{18,19} reflecting their chemical similarity in the solid state.

We then developed a model for the *a*-Si_{*x*}Ge_{1-*x*} alloy by decorating, with probabilities *x* and 1-*x*, the sites of our *a*-Si structure with Si or Ge atoms having masses M_{Si} and M_{Ge} , respectively ($M_{\text{Ge}}/M_{\text{Si}}=2.58$). As a first approximation we used a "mean-field approximation," in which the force constants α of all bonds have the same value for a given *x*, with the value being the mean α in the network. This simplified the calculations significantly and eliminated the need to make added approximations about the Si-Ge bond-stretching force constant. This assumption was justified *a posteriori* by the fact that the difference in masses alone provides good agreement with the available experimental data. As a further test of the

alloy model we also calculated the vibrational DOS for *a*-Si/*a*-Ge superlattices, using different values of α for Si-Si bonds and Ge-Ge bonds, together with a mean α for the Si-Ge bond. Results were very similar to those with the mean α for all atoms.

III. *a*-Si_{*x*}Ge_{1-*x*} ALLOYS

Experimental Raman measurements of the vibrational spectra of *a*-Si_{*x*}Ge_{1-*x*} alloys, made by Lannin,¹ are summarized in Fig. 2. It is evident that the alloy spectra do not interpolate smoothly between the *a*-Si and *a*-Ge data. The high-frequency DOS (above 200 cm⁻¹) splits into three distinct vibrational bands for the *x*=0.5 and *x*=0.3 alloys. The 390-cm⁻¹ band is clearly absent in either *a*-Si or *a*-Ge, and is most prominent for *a*-Si_{0.5}Ge_{0.5}. The growth of this new band is also indicated as a small feature in the data for the *x*=0.7 and *x*=0.1 alloys. The low-frequency DOS peak shifts uniformly between the values for *a*-Si and *a*-Ge. The new 390-cm⁻¹ band was taken to represent the vibrations of the Si-Ge bonds, whereas the other two high-frequency peaks were assigned to Si-Si and Ge-Ge bond-stretching vibrations. We show explicitly that our calculations support this interpretation. The Raman measurements represent a convolution of the actual DOS with a frequency-dependent scattering cross section that varies as $\sim\omega^2$ at low frequencies.¹ This suppresses the heights of the lower-frequency transverse-acoustical (TA) peak in the Raman spectra relative to the calculated values.

Our results for the vibrational DOS of the alloys (Fig. 2) model the trends shown by the experimental measurements for all values of *x*. The calculations clearly show the three-peak feature in the higher-frequency DOS for Si concentrations *x* of 0.3 and 0.5. The peak at 382 cm⁻¹, assigned to the Si-Ge vibration, compares well with the experimental value^{1,3} of 390 cm⁻¹, and is most prominent for the *x*=0.5 alloy. A small feature at 382 cm⁻¹ is also present in the calculation at *x*=0.1, similar to the experimental data.¹

We characterized the alloy vibrations by calculating the projected densities of states projected on the three types of bonds in the system (Fig. 3), and the DOS pro-

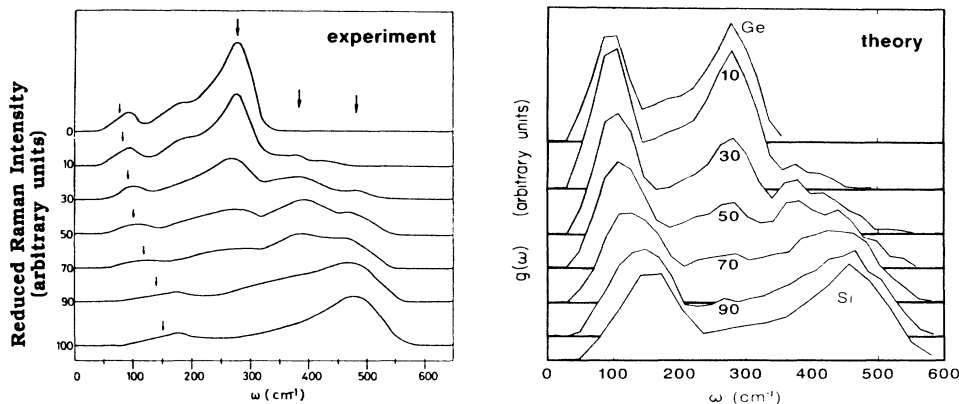


FIG. 2. Vibrational densities of states for *a*-Si_{*x*}Ge_{1-*x*} alloys calculated from our model (right panel), compared with reduced Raman scattering spectra (left panel) obtained by Lannin (Ref. 1).

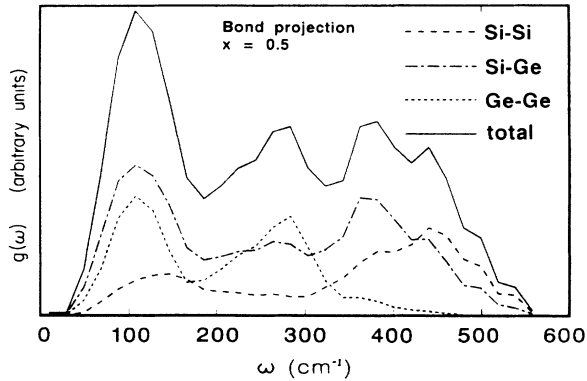


FIG. 3. Bond-projected partial densities of states for $a\text{-Si}_{0.5}\text{Ge}_{0.5}$. The solid line is the total density of states.

jected on the sites (Fig. 4), for $\text{Si}_{0.5}\text{Ge}_{0.5}$. Also shown in Figs. 3 and 4 is the total DOS which has peaks at 108, 284, 382, and 440 cm^{-1} . The bond-projected DOS for bonds of type XY (X, Y are Si or Ge) was defined as

$$g^{XY}(\omega) = \sum_n \delta(\omega - \omega_n) \frac{\sum_{ij}^{(ij)=XY} (\mathbf{u}_i - \mathbf{u}_j) \cdot (\mathbf{u}_i - \mathbf{u}_j)}{\sum_{i \neq j} (\mathbf{u}_i - \mathbf{u}_j) \cdot (\mathbf{u}_i - \mathbf{u}_j)}. \quad (2)$$

\mathbf{u}_i is the displacement of atom i from its equilibrium position for the mode with frequency ω_n . The sum in the denominator is over all the nearest-neighbor atom pairs i, j .

It is clear that the projected DOS on Si—Ge bonds (Fig. 3) has a strong peak at 382 cm^{-1} confirming that the feature at this frequency arises primarily from Si—Ge bond-stretching motions. Projections on the Si—Si and Ge—Ge bonds indicate that the vibrational bands at 284 and 440 cm^{-1} can be assigned to vibrations of Si—Si and Ge—Ge bonds, respectively.

Further information on the nature of the vibrational bands may be obtained from a calculation of the projected DOS in the Si and Ge sites (Fig. 4). As expected the Si-Si and Ge-Ge vibration bands gives rise to peaks in the

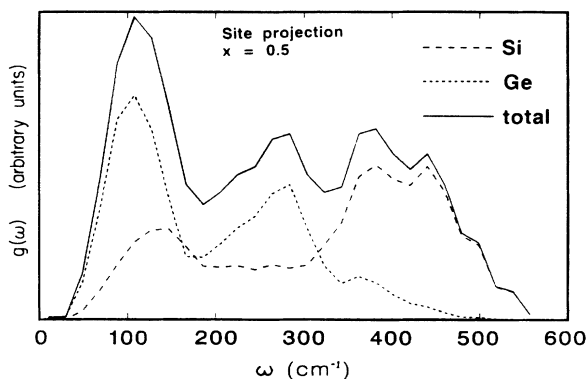


FIG. 4. Site-projected partial densities of states for $a\text{-Si}_{0.5}\text{Ge}_{0.5}$. The solid line is the total density of states.

Si and Ge site projections. At 382 cm^{-1} there is a strong peak in the Si site projection and a much weaker peak in the Ge site projections. This is physically reasonable since 382 cm^{-1} lies beyond the maximum frequency for pure $a\text{-Ge}$, and modes of this frequency can have large amplitudes of vibration for the lighter Si atoms, but not for the heavier Ge atoms.

Very similar properties for the amorphous silicon-germanium alloy DOS, the localization characteristics, and the features of the Si—Ge bond-stretching band were found with a model that used different equilibrium bond lengths for the Si—Si, Ge—Ge, and Si—Ge bonds (2.351, 2.40, and 2.45 Å, respectively). Also the DOS for pure $a\text{-Ge}$ was insensitive to having a equilibrium bond length that was the Si value (2.351 Å) or the experimental Ge—Ge value (2.447 Å). This indicated that the alloy disorder was adequately modeled by combination of mass disorder and structural disorder of our model, and that the additional disorder from having different bond lengths was not necessary. In view of the insensitivity of the calculations to the Ge—Ge bond length, we chose, for simplicity, the equilibrium Ge—Ge bond length to be the same as that for Si. As a further test of our calculations we performed calculations using the WWW $a\text{-Si}$ network and obtained very similar results for the alloy vibrational densities of states and high-frequency localization that is discussed later in this section.

We do emphasize that our calculated DOS cannot be exactly compared to the Raman data because of the frequency-dependent Raman coupling constant that is convoluted with the Raman data. However, it has been argued¹ that the frequency dependence of this Raman coupling constant is sufficiently weak that the Raman data is a reasonable representation of the actual DOS. A calculation of the Raman matrix elements and the Raman spectra seemed unwarranted since we could identify all the essential physical features of the data with our calculated DOS.

The frequencies of the three bond-stretching vibrational bands have been obtained in a five-atom Bethe-lattice calculation,²⁰ but the form of the alloy $g(\omega)$ did not compare well with experiment¹ owing to the simplified model employed. The present calculations compare well with the experimental $g(\omega)$ for all x . To the best of our knowledge, the present work represents the only calculation of the localization properties of the amorphous alloys, which we shall now describe.

In this section we are especially interested in seeing how the spatial localization of the vibrational states is affected by the mass disorder in the random alloys $a\text{-Si}_x\text{Ge}_{1-x}$. In the next section similar considerations pertaining to layering in $a\text{-Si}/a\text{-Ge}$ superlattices will be discussed. The degree to which each vibrational mode is either localized or extended in nature can be characterized by its inverse participation ratio,^{21,22} defined for each eigenmode as

$$p^{-1} = \sum_j (\mathbf{u}_j \cdot \mathbf{u}_j)^2 / \left[\sum_j \mathbf{u}_j \cdot \mathbf{u}_j \right]^2, \quad (3)$$

where \mathbf{u}_j is the displacement of atom j from its equilibrium position. The definition (1) implies that spatially ex-

tended modes have small values of p^{-1} , on the order of $1/N$, N being the number of atoms in the system, whereas localized modes have large ratios that can reach a maximum value of 1 for a mode completely localized on a single atom. Results for a -Si are shown in Fig. 5 (lower panel, $x = 1$).

In our previous studies of amorphous silicon,⁸ very strong localization was found for modes at the high- and low-frequency edges of the vibrational spectrum. The novel localization phenomena at low frequencies were due to the presence of undercoordinated atoms. No such effects were found for amorphous-silicon models that had only fourfold-coordinated atoms. Allowing for the hybridization between localized and extended states at low

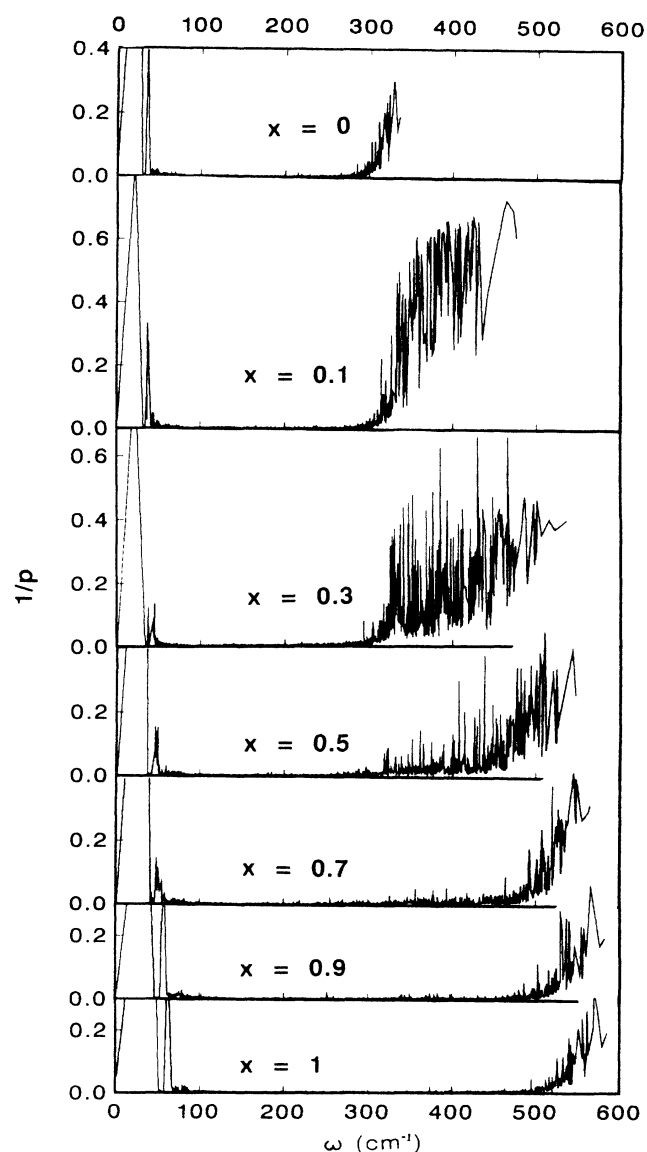


FIG. 5. Inverse participation ratios p^{-1} , which characterize the localization of vibrational modes, in a -Si _{x} Ge _{$1-x$} . Strongly low-frequency resonant modes are fully shown for $x = 0.1$, but are off scale for other x . The low-frequency behavior for all x is very similar to the $x = 0.1$ case.

frequencies leads to the formation of strongly resonant states⁸ for the low-frequency modes with large p^{-1} values. These resonant states have eigenfunctions that exponentially decay away from the defect sites and have strong scattering properties that are usually attributed to localized states. Henceforth, we will refer to these low-frequency modes with large p^{-1} as resonant instead of localized.

In our previous work,⁸ localized modes at the high-frequency band edge were found in both the BGS models as well as in the WWW a -Si model that had only fourfold-coordinated atoms. The localization was considerably enhanced by the presence of fivefold-coordinated sites. The p^{-1} values for the a -Si model are plotted in Fig. 5 ($x = 1$ panel).

The effect of mass disorder in the alloy on the localization is illustrated in Fig. 5, for Si _{x} Ge _{$1-x$} , for x varying between 0 and 1. The localization of the high-frequency modes is strongly enhanced in both magnitude and frequency range in the alloy as compared to the pure amorphous materials. Most significantly, there is a dramatic increase in the number and magnitude of localized states in the $x = 0.1$ alloy in comparison to a -Ge. All the vibrational modes above 300 cm^{-1} are strongly localized for $x = 0.1$. This situation occurs because these high-energy modes are primarily vibrations of the lighter Si atoms in bond-stretching Si-Si or Si-Ge motions. For small x , these high-frequency modes cannot propagate through a structure consisting mostly of much heavier Ge atoms. As x increases, the high-frequency modes are increasingly able to propagate through neighboring Si sites, and the localization decreases in magnitude. A large number of the modes above 300 cm^{-1} become extended for $x > 0.5$, and the mobility edge shifts near the Si band edge to $\sim 500 \text{ cm}^{-1}$ for $x \geq 0.9$.

The low-frequency resonant modes of the alloy can be enhanced or suppressed relative to the a -Si case, depending on whether the atom with a large vibrational amplitude is Si or Ge. Here too, localization is enhanced if the neighboring sites of the vibrating atom are unlike atoms. In Fig. 5 we note an enhanced inverse participation ratio of the resonant 6-meV mode but a suppression for the resonant 8-meV modes, for $x = 0.5$ as compared to a -Si. The 6-meV mode is primarily a vibration of a threefold-bonded atom, whereas the 8-meV mode involves vibrations of both threefold- and fourfold-bonded atoms. The form of the p^{-1} for these resonant modes is similar for all x .

IV. a -Si/ a -Ge SUPERLATTICES

Another class of amorphous Si-Ge systems that has attracted recent attention comprises the periodic superlattices of alternating a -Si and a -Ge layers. Superlattices with repeat distances as small as 8 Å have been grown by plasma-assisted chemical vapor deposition. These are interesting systems for studies of amorphous interfaces, and the nature of vibrational modes at these interfaces. An important issue is whether these layered structures can be fabricated with sharp interfaces, an issue which has been addressed in detailed Raman scattering investigations.^{4,5} Shown in Fig. 6 are Raman measurements for superlat-

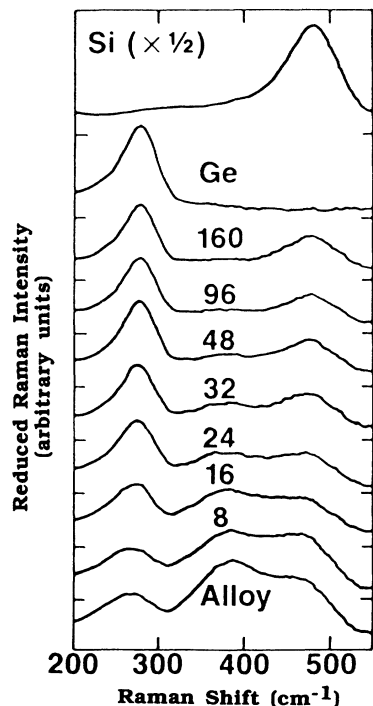


FIG. 6. Reduced Raman spectra for *a*-Si/*a*-Ge superlattices with repeat distance d_r in Å as marked, obtained by Persans *et al.* (Ref. 3). Also shown for reference are Raman spectra for *a*-Si, *a*-Ge (upper part), and *a*-Si_{0.55}Ge_{0.45} (lower part).

tices with varying repeat distances d_r , made by Persans, Ruppert, Abeles, Tiedje, and Stasiewski.^{4,5} The Raman data indicate that for superlattices with period $d_r > 40$ Å, the DOS is a superposition of the separate *a*-Si and *a*-Ge DOS. For thinner superlattices ($d_r < 30$ Å), a strong vibrational band corresponding to Si—Ge bond-stretching motions is present. At the smallest superlattice period of 8 Å, the Si—Ge and Si—Si bands have approximately equal intensity, and the DOS is qualitatively similar to that of the alloy. These observations were interpreted^{4,5} as suggesting a superlattice structure with an interface consisting of one monolayer of randomly mixed Si and Ge, bounded by pure materials.

We have investigated this interpretation closely, by constructing *a*-Si/*a*-Ge superlattices with period $d_r = 16.3$ Å (Fig. 7) with different widths r , of a roughened interface layer and performing DOS calculations for the superlattices. The *a*-Si/*a*-Ge superlattice (labeled $r = 0$ in Fig. 7) was constructed by inserting geometrical planes spaced $d_r/2$ apart into the amorphous network. The planes could be chosen to be perpendicular to any of the three Cartesian directions, and for any orientation the positions of the planes, i.e., the amorphous layers, could also be varied. Atoms on either side of the plane were chosen to be either Si or Ge. For the $r = 0$ superlattice, the interface between the *a*-Si and *a*-Ge layers was “sharp,” i.e., geometrically defined—no intermixing of the Si and Ge was permitted. Of course, each interface has an intrinsic roughness of approximately a bond length. Calculations using the 216-atom BGS

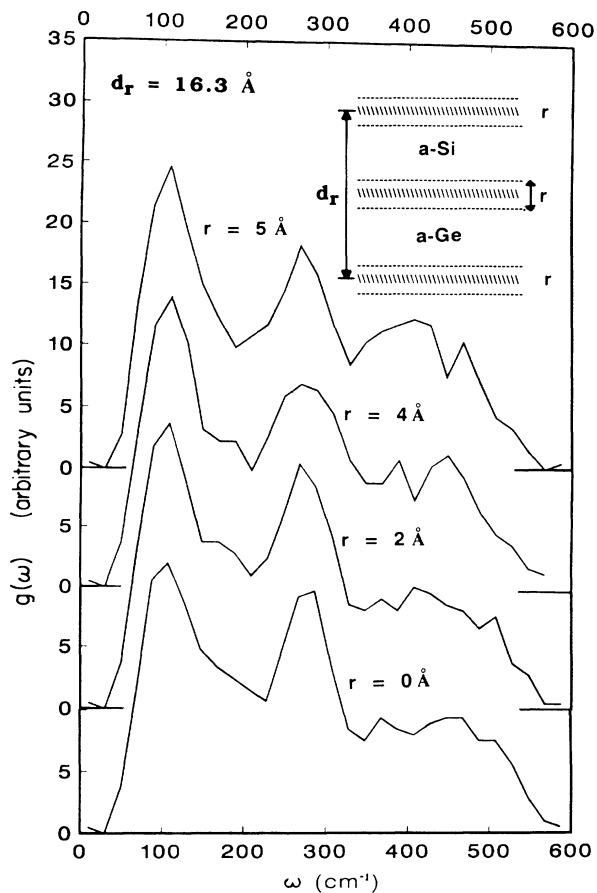


FIG. 7. Calculated vibrational densities of states for *a*-Si/*a*-Ge superlattices with repeat distance $d_r = 16.3$ Å. Calculations are for different widths r (in Å) of interface regions where the Si and Ge were allowed to intermix equally.

model were compared with the Raman measurements for approximately the same d_r . As is evident from Fig. 7, the spectra of the *a*-Si/*a*-Ge superlattice with a geometrically defined interface ($r = 0$) did not produce the Si—Ge bond-stretching feature at ~ 370 cm⁻¹ found experimentally. There was a strong Ge—Ge stretch band, but the Si—Ge and Si—Si stretch modes coalesced into a broad feature.

Interfacial roughening effects were incorporated by allowing the Si and Ge atoms to intermix equally within a region of width r ($r = 2.0, 4.0,$ and 5.0 Å) at each interface. This interfacial region is microscopically similar to *a*-Si_{0.5}Ge_{0.5} alloy. Roughened interfaces wider than 5.0 Å were not considered here, since the individual layer widths are only 8.15 Å in the model. In the results of Fig. 7, the Si-Ge feature is absent for $r = 2.0$ Å but is clearly present for the roughened interfaces with widths $r = 4.0$ and 5.0 Å. In fact, for $r = 4.0$ and 5.0 Å, there are the three distinct peaks corresponding to the Ge—Ge, Si—Ge, and Si—Si stretch modes, a feature qualitatively similar to the Raman data. We interpret our results to indicate that a roughened interfacial layer of 4–6 Å is needed to model the experimentally observed spectra. Roughening widths of 2–3 Å appear too small to account

for the data. The results for the roughened interface of width 2.0 Å are qualitatively similar to those of the unroughened interface. We interpret this as due to the amorphous interfaces having an intrinsic roughness of the order of ~ 2 Å. This is supported by the fraction of Si—Ge bonds being similar for the $r=2.0$ Å system (20%), and the unroughened superlattice (16%). For $r=5$ Å there are as many as 36–40 % of Si—Ge bonds in the system.

We also performed DOS calculations for amorphous superlattices that had (i) different positions of the interfaces constructed by translating the lattice planes, (ii) interfacial planes perpendicular to other Cartesian directions. We also constructed a -Si/ a -Ge superlattices from the WWW amorphous network¹⁰ in which all atoms were fourfold coordinated. DOS calculations for all these different cases led to similar conclusions that roughened interfacial layers of width 4–6 Å were needed to account for the Raman data.

We found that the experimental spectra could also be accounted for by having geometrically sharp interfaces between the amorphous layers, but allowing some homogeneous intermixing of the Ge (Si) into the a -Si (a -Ge) layer. For a superlattice of a -Si_{*y*}Ge_{1-*y*}/ a -Si_{1-*y*}Ge_{*y*} with $y=0.7$, 49% of the bonds are of the Si—Ge type, and calculated results for this superlattice are similar to that for the $r=5.0$ Å interfacial roughening. Superlattices with $y > 0.80$ did not yield strong Si-Ge features. Whether this form of intermixing actually occurs depends on the diffusion constants under the experimental growth conditions employed.

As our calculations indicate, Raman spectroscopy is indeed a sensitive probe of structural properties and interface sharpness. Fabrication of a -Si/ a -Ge superlattices with much sharper atomically abrupt interfaces have recently been reported,²³ using a technique in which the plasma was interrupted for several seconds after growth of each layer, to allow adequate time for the exchange of the SiH₄, GeH₄ and H₂ constituent gases. Previously, the a -Si/ a -Ge superlattices^{4,5} were grown by plasma-assisted chemical vapor deposition where the constituent gases were rapidly switched without interrupting the plasma. Theoretical analysis, along the lines of this paper, of the sharper a -Si/ a -Ge superlattices is feasible if vibrational spectra measurements are available.

The localization characteristics of the superlattice modes can be illustrated by the calculated inverse participation ratios, projected on atoms at the interface and on atoms in the pure amorphous layers, defined by

$$p_a^{-1} = (N/N_a) \sum_j^a (\mathbf{u}_j \cdot \mathbf{u}_j)^2. \quad (4)$$

The sum is over all atoms of type a , where a represents either atoms at the interface or in the amorphous layers. N_a is the number of atoms of that type, and N the total number of atoms. The eigenvectors are assumed to be normalized to 1 over all the atoms. Results for the projected inverse participation ratios, together with the total p^{-1} , are shown in Fig. 8 for the $r=0$ case (sharp inter-

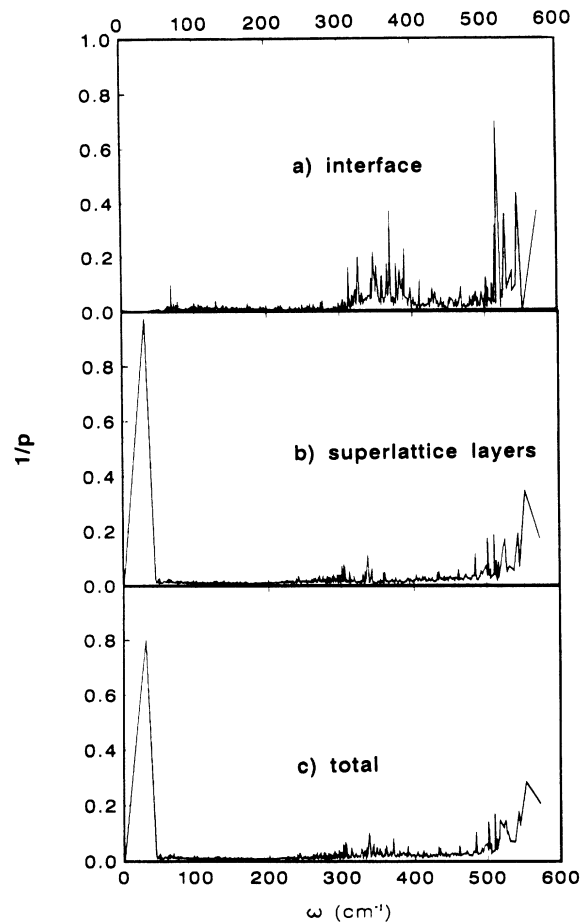


FIG. 8. Inverse participation ratios for the a -Si/ a -Ge superlattice projected on interface atoms and sites in the individual amorphous layers. The total inverse participation ratios are also shown for comparison.

face).

The low-frequency localization phenomena is entirely confined to the individual layers. The high-frequency localized modes primarily reside on the interface atoms, where the disorder is large and locally similar to the alloy.

V. SUMMARY

The calculations presented in this paper deal with vibrational densities of states and vibrational localization in a -Si_{*x*}Ge_{1-*x*} alloys and a -Si/ a -Ge superlattices. The alloys are disordered in two senses, i.e., not only are the atomic sites arranged in an aperiodic structure, but also the identity of the atoms can be randomly either Si or Ge. The latter effect, in terms of the vibrational problem, can be considered mass disorder because of the chemical similarity of the atoms. The densities of states above 70 cm⁻¹ for the alloys seem to comprise two kinds of modes, those with frequencies below a frequency of about 290 cm⁻¹ and those of higher frequency. The lower-frequency modes are spatially extended, and the features of the densities of states scale smoothly with concentration between

Si and Ge. The higher-frequency modes are spatially localized, and the major contributions to the high-frequency densities of states are peaks due to Si—Si, Si—Ge, and Ge—Ge bond-stretching motions.

The densities of states for the superlattices can be either like a weighted sum of those for *a*-Si and *a*-Ge, or like an amorphous alloy spectrum, depending on the thickness of the layers, and the degree of Si-Ge intermixing at the layer interfaces. The distributions differ mainly in the strength around 380 cm^{-1} , where the Si—Ge bond-stretching modes occur. The weight of the 380-cm^{-1} feature thus serves as a convenient measure of the number of Si—Ge bonds. Comparison with published Raman spectra^{4,5} indicates that the intermixed region in the measured samples was about 4–6 Å thick, i.e., thin but not atomically thin. Localized modes in the superlat-

tices are primarily high-frequency modes confined to the interfacial regions.

ACKNOWLEDGMENTS

We thank J. Lannin and P. Persans for helpful discussions of their experimental work. We acknowledge support from the Air Force Office of Scientific Research for work performed at the Microelectronics Research Center, and from the National Science Foundation for a grant of supercomputer time at the National Center for Supercomputer Applications, Champaign, Illinois. Work at The Ames Laboratory, operated by Iowa State University for the U.S. Department of Energy (U.S. DOE) under Contract No. W-7405-eng-82, was supported by the Director for Energy Research, Division of Materials Sciences, U.S. DOE.

¹J. S. Lannin, *Amorphous and Liquid Semiconductors* (Taylor and Francis, London, 1974), p. 1245.

²J. S. Lannin (private communication), and unpublished.

³N. J. Shevchik, J. S. Lannin, and J. Tejada, *Phys. Rev. B* **7**, 3987 (1973).

⁴P. D. Persans, A. F. Ruppert, B. Abeles, T. Tiedje, and H. Stasiewski, *Phys. Rev. B* **32**, 5558 (1985).

⁵P. D. Persans, A. F. Ruppert, B. Abeles, T. Tiedje, and H. Stasiewski, *J. Phys. (Paris) Colloq.* **8**, (597) (1985).

⁶R. Biswas, G. S. Grest, and C. M. Soukoulis, *Phys. Rev. B* **36**, 7437 (1987).

⁷R. Biswas and D. R. Hamann, *Phys. Rev. B* **36**, 6434 (1987); *Phys. Rev. Lett.* **55**, 2001 (1985).

⁸R. Biswas, A. M. Bouchard, W. Kamitakahara, C. M. Soukoulis, and G. S. Grest, *Phys. Rev. Lett.* **60**, 2280 (1988).

⁹W. A. Kamitakahara, C. M. Soukoulis, H. R. Shanks, U. Buchenau, and G. S. Grest, *Phys. Rev. B* **36**, 6539 (1987).

¹⁰F. Wooten, K. Winer, and D. Weaire, *Phys. Rev. Lett.* **54**, 1392 (1985).

¹¹K. Winer, *Phys. Rev. B* **35**, 2366 (1987).

¹²W. D. Luedtke and U. Landman, *Phys. Rev. B* **37**, 4656 (1988).

¹³M. D. Kluge, J. Ray and A. Rahman, *Phys. Rev. B* **36**, 4234 (1987).

¹⁴R. Car and M. Parinello, *Phys. Rev. Lett.* **60**, 204 (1988).

¹⁵P. N. Keating, *Phys. Rev.* **145**, 637 (1966).

¹⁶K. Ishii, M. Kumeda, and T. Shimuzu, *Solid State Commun.* **50**, 367 (1984).

¹⁷G. Baraff, E. O. Kane, and M. Schluter, *Phys. Rev. B* **21**, 5662 (1980).

¹⁸W. Weber, *Phys. Rev. B* **15**, 4789 (1977).

¹⁹G. Nilsson and G. Nelin, *Phys. Rev. B* **6**, 3777 (1972).

²⁰B. K. Agarwal, *Solid State Commun.* **37**, 271 (1981).

²¹R. J. Bell, *Rep. Prog. Phys.* **35**, 1315 (1975).

²²P. Dean, *Rev. Mod. Phys.* **44**, 127 (1972).

²³F. Sette, B. Abeles, L. Yang, A. A. MacDowell, C. H. Richardson, and D. Norman, *Phys. Rev. B* **37**, 2749 (1988).